Title

Simulating International Drought Experiment field observations using the Community Land Model

Authors

Hilton, Timothy W

Loik, Michael E

Campbell, J Elliott

Publication Date

2019-03-01

DOI

10.1016/j.agrformet.2018.12.016

Agricultural and Forest Meteorology 266–267 (2019) 173–183

Contents lists available at ScienceDirect

Agricultural and Forest Meteorology

journal homepage: www.elsevier.com/locate/agrformet

Simulating International Drought Experiment field observations using the Community Land Model

Timothy W. Hilton[a,*], Michael E. Loik[b], J. Elliott Campbell[a,1]

[a] Sierra Nevada Research Institute, University of California, Merced, Merced, CA, USA
[b] Environmental Studies Department, University of California, Santa Cruz, Santa Cruz, CA, USA

ARTICLE INFO

Keywords:
Drought
GPP
Community Land Model
CLM
International Drought Experiment
IDE

ABSTRACT

Anthropogenic climate change will alter regional hydrologic cycles around the world, in part by increasing the frequency or duration of droughts in some areas. The International Drought Experiment (IDE) is investigating the impact of severe drought on terrestrial vegetation by experimentally reducing precipitation at dozens of sites. Here we implement the IDE precipitation reduction protocol using the Community Land Model (CLM). Though many model results suggest that carbon fertilization will outpace drought-caused reduction of terrestrial carbon uptake, uncertainty is large. We therefore configure CLM to consider carbon cycling impacts of reduced moisture availability without intertwining the effects of carbon fertilization or phenological changes. California hosts a number of IDE sites and a wide range of topography, climate, and biomes. CMIP5 predictions suggest 21st century California will experience droughts in excess of the 1000-year climatological record for both frequency and magnitude. CLM suggests that some regions, including much of Northern California, may experience a steeper decline in gross primary productivity (GPP) during 21st century severe droughts than during 20th century severe droughts. Vegetation in Northern California experiences virtually all of this GPP reduction during the dry season, with little wet season GPP reduction even during severe drought. Southern California vegetation experiences soil moisture GPP limitation at virtually all times, increasing substantially with drought severity. Southern California should experience a more pronounced shift in GPP seasonality and decline in magnitude relative to Northern California during droughts. Some parts of every vegetated continent see changes to drought response and seasonality similar to Southern California. Our CLM results provide drought impacts that forthcoming IDE field observations may test, can help to spatially upscale site-based IDE observations of drought impact, and provide CLM's prediction of reduced precipitation impacts per unit leaf area index.

1. Introduction

Anthropogenic climate change is already profoundly altering local, regional and global circulation, and will affect weather and climate in the 21st century relative to 20th century norms (IPCC, 2013). Implications include critical alteration of regional hydrologic cycles relative to the 20th century (Collins et al., 2013; Trenberth et al., 2014; Dai, 2012; Prudhomme et al., 2014). Indeed, recent analyses suggest it is not out of the question that such changes are underway and detectable (Dai, 2012; Prein et al., 2016). The Coupled Model Intercomparison Project Phase 5 (CMIP5) ensemble of tens of general circulation models consistently predict drier soil conditions around the Mediterranean, parts of South America, southern Africa, and the Southwest USA. These drier soils are forced by changes in precipitation supply, as well as evaporative demand due to higher air temperatures (Collins et al., 2013).

Effects of drought may include changes in ecological succession (Clark et al., 2016; Fauset et al., 2012), widespread plant mortality (Anderegg et al., 2016; McDowell et al., 2015), and physiological changes within plants that affect gross photosynthetic productivity (GPP) and carbon cycling (Hogg et al., 2008; Zhao and Running, 2010; McDowell et al., 2015). Carbon dioxide (CO_2) fertilization is likely to at least partially offset drought-driven GPP decline (Swann et al., 2016) for at least some regions of the world and all CMIP5 models consistently predict increased future global GPP, although considerable uncertainty exists surrounding the magnitude and spatial behavior of that increase (Friedlingstein et al., 2014; Reichstein et al., 2013; Schimel et al., 2015; Liu et al., 2016). This uncertainty, the potential of disturbances such as

* Corresponding author at: Environmental Studies Department, University of California, Santa Cruz, 1156 High Street (ENVS Mailstop), Santa Cruz, CA 95064, USA.
E-mail address: twhilton@ucsc.edu (T.W. Hilton).
[1] Present address: Environmental Studies Department, University of California, Santa Cruz, Santa Cruz, CA, USA.

https://doi.org/10.1016/j.agrformet.2018.12.016
Received 17 July 2018; Received in revised form 27 November 2018; Accepted 21 December 2018

droughts to limit or offset carbon fertilization-driven increase in the terrestrial CO_2 sink (Reichstein et al., 2013), and the IDE occurring now (in present, not future, CO_2 levels) make it useful to study drought impacts in isolation of carbon fertilization.

Field studies or remote sensing provide indispensable knowledge but are poorly suited to the problem of separating drought-driven carbon cycle changes from changes driven by carbon fertilization. Single-site field studies of fundamental relationships between precipitation and ecology provide crucial mechanistic linkages between soil water availability and plant, community and ecosystem responses, but they are limited to relatively small spatial areas and short time scales (Ogle et al., 2015). Distributed experiments can help identify emergent properties and unifying principles across larger spatial scales (Knapp et al., 2017). Upscaling such experiments to landscape-scale is difficult because land surface heterogeneity causes many drought impacts to be highly localized (Reed and Loik, 2016; Assal et al., 2016). Remote sensing methods offer a far greater spatial perspective, but it is challenging to separate long-term structural ecosystem changes from phenological changes forced by interannual climate variability (Assal et al., 2016).

In contrast to field observations and remote sensing, ecosystem models provide a framework to scale site-based observations and interpret remote sensing data from a process-based perspective (Schaefer et al., 2012; Hilton et al., 2014). Here we present a set of land surface model experiments using the Community Land Model (CLM) (Oleson et al., 2010) version 4.0, using forcings (described in detail in Section 2) consistent with the International Drought Experiment (IDE). The IDE (http://www.drought-net.org) is a research coordination network to quantify sensitivity of biodiversity and above-ground productivity to drought for terrestrial ecosystems around the world. The goal of our experiments was to identify emergent properties across time and space, and to help generate hypotheses by which the IDE site-level experiments may test CLM. Many published studies have examined CLM's performance in reproducing observations and have identified important biases, and we do not seek here to extend these studies. We examine instead the differences between CLM simulations driven by “standard” atmospheric data and simulations driven by the IDE forcings. This differencing approach should allow the known CLM biases to cancel one another, while preserving the effects of meteorological drought. We focused on California IDE sites to help interpret future IDE observations, and to help upscale IDE results to regional or global scales.

California IDE sites have tremendous biological diversity that is driven in part by climatic differences across the state. Yet biological diversity and productivity are constrained by several factors: California receives most of its annual precipitation in the winter months, interannual variability in precipitation is quite high, the amount of precipitation is generally higher for Northern compared to Southern California, there are substantial coast-to-inland gradients of temperature and precipitation, and drought is enhanced statewide by increasingly warmer atmospheric temperatures. Regional analyses of the Southwest USA suggest that the hydrologic cycle of the next 100 years is likely to change significantly relative to the 20th century (Cook et al., 2015; Wuebbles et al., 2014; Seager et al., 2013, 2007; Seager and Vecchi, 2010). The CMIP5 ensemble predicts an increase in winter (January, February, March) precipitation for the northern half of California, and decreased precipitation there during all other seasons and in the southern half of the state in all seasons (Seager et al., 2013). However the predicted Northern California winter precipitation increase is counterbalanced by increased temperatures from radiatively forced warming, causing concurrent increased evaporation in excess of precipitation gains. Thus, the CMIP5 ensemble strongly trend toward significantly less moisture available to plants throughout California during the 21st century relative to CMIP5 simulations spanning the years 1850–2000 (Seager et al., 2013; Cook et al., 2015) (though the models are not unanimous (Cheng et al., 2016) and uncertainty is non-trivial (Mankin et al., 2017)). These projected 21st century droughts are also more severe than any historical droughts in the North American Drought Atlas (NADA) 1000-year paleoclimate reconstruction from tree ring data (Cook et al., 2015). Observed precipitation from 1980 to 2010 suggests that the 21st century drying trend predicted for California by the CMIP5 model ensemble is underway (Prein et al., 2016). Furthermore, the observed drying is driven by decreased frequency of precipitation-causing weather patterns – a change in the base state of the climate – and not decreased intensity of individual precipitation events, which would be more attributable to natural variability (Prein et al., 2016).

The past several years in California have exhibited many of these predicted changes, with the state experiencing a drought not seen for 700–1200 years (Robeson, 2015; Griffin and Anchukaitis, 2014) during 2012–2015. The drought was immediately followed by the third-highest October to April precipitation total since 1895 (NOAA National Centers for Environmental Information, 2017), restoring by May 2017 statewide snowpack and reservoir levels to 180% and 110%, respectively, of their 1979–2015 averages (up from 2% and 65%, respectively, in May 2015) (Cal. Dept. of Water Resources, 2017).

The precipitation we used to drive our model results simulates the IDE precipitation reduction protocol and spans the wide range of extreme hydrological swings that California has recently experienced. In light of this and the hydrological changes predicted for California and the Southwest USA, we identify slope changes in the photosynthetic productivity (gross primary productivity, GPP) response to precipitation. We analyze these changes in our simulations for eight field stations on a North-South spatial transect across California and then apply them globally.

2. Materials and methods

The IDE protocol prescribes a universal rainfall interception methodology for all sites, consisting of adjacent experimental and control plots. At each site the annual proportion of precipitation allowed to reach the ground is determined from 100-year records of annual precipitation – roughly creating the one-year-in-one hundred-years drought. We focus on eight California locations (Fig. 1, Table 1) to examine our CLM results: five University of California Natural Reserve System (UCNRS) sites (Younger Lagoon Reserve, McLaughlin Reserve, Sedgwick Reserve, Box Springs Reserve, Sierra Nevada Aquatic Research Laboratory (SNARL)), as well as Loma Ridge Global Change Experiment, Sierra Foothill Research Extension Center, and Carrizo Plain. We also examine three heavily studied more easterly sites in North America (Table 1) to provide context for the California sites.

We used the Community Earth System Model (CESM) (CESM Software Engineering Group (CSEG), 2013) to generate scenarios of GPP for 1-in-100 year extreme droughts corresponding to the IDE. CESM is a coupled global climate model developed to address research questions about the interactions of Earth's atmosphere, oceans, cryosphere, and biogeochemical systems. CLM is the land surface component of the CESM.

Version 4.0 of CLM (Oleson et al., 2010) may be run with or without prognostic carbon and nitrogen pool simulations and may be run coupled or uncoupled from an atmospheric model (Lawrence et al., 2011). When uncoupled from the atmosphere, a prescribed and static “data atmosphere” drives land surface processes. In this offline mode, land surface processes are affected by the atmosphere, but the atmosphere is unaffected by land surface processes. When run without prognostic carbon and nitrogen pools, observations from the satellite-borne Moderate Resolution Imaging Spectroradiometer (MODIS) are used to prescribe seasonal leaf area indices, stem area indices, and vegetation height (Lawrence et al., 2011). This CLM configuration is conventionally (and hereafter) referred to as CLM4SP (version 4.0, Satellite Phenology).

We conducted two 15 model-year CLM4SP simulations: a control run and an experimental run. Both runs used a horizontal resolution of

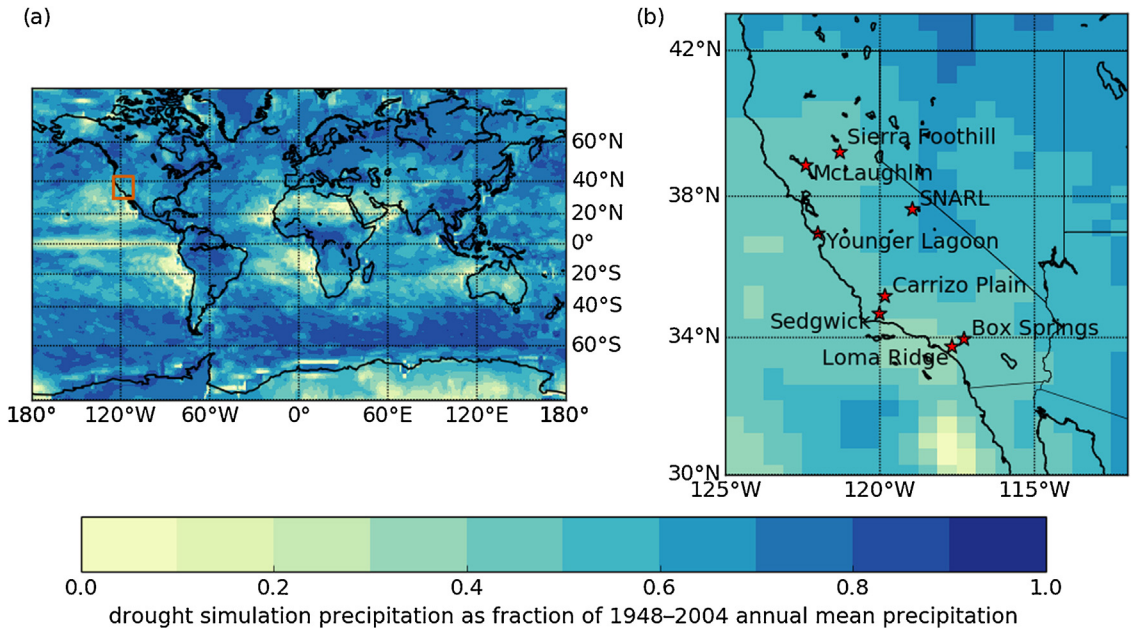

Fig. 1. International Drought Experiment (IDE) per-gridcell precipitation reduction. Panel (a): global precipitation reduction as a fraction of the 1948–2004 annual mean total precipitation. Panel (b): as panel (a), but zoomed to the California, USA analysis area (shown in the orange box in panel (a)). Precipitation reduction fractions are calculated as ((1st percentile)/(50th percentile)) of the 1948–2004 (Qian et al., 2006) annual total precipitation (see Section 2). Red stars on the panel (b) denote the California analysis sites described in Table 1. (For interpretation of the references to color in this figure legend, the reader is referred to the web version of this article.)

Table 1
Locations used for model evaluation (see also Fig. 1b).

	Latitude	Longitude	Reference
Site (California, USA)			
Younger Lagoon Reserve	36.97° N	122.03° W	Reed et al. (2011)
McLaughlin Reserve	38.87° N	122.43° W	http://nrs.ucdavis.edu/McL/
Sedgwick Reserve	34.70° N	120.02° W	http://sedgwick.nrs.ucsb.edu/
Box Springs Reserve	33.98° N	117.30° W	http://www.ucnrs.org/
Loma Ridge Global Change Experiment	33.73° N	117.70° W	Nelson et al. (2015)
Sierra Foothill Research Extension Center	39.25° N	121.28° W	Millikin and Bledsoe (1999)
Carrizo Plains National Monument	35.19° N	119.86°	Buck-Diaz and Evens (2011)
Sierra Nevada Aquatic Research Laboratory (SNARL)	37.61° N	118.83° W	Reed and Loik (2016)
Site (Central/East USA)			
Harvard Forest	42.54° N	72.17 ° W	Urbanski et al. (2007)
WLEF	45.95° N	90.27° W	Davis et al. (2003)
ARM Southern Great Plains	36.61° N	97.49° W	Fischer et al. (2007)

0.47 by 0.63 degrees and were driven by a “data atmosphere” (compset I_2000). The two runs differed only in the magnitudes of precipitation events.

CLM-simulated carbon fluxes have been compared extensively to eddy covariance observations both globally and regionally (e.g. Stöckli et al., 2008; Lawrence et al., 2011; Bonan et al., 2011) as well as locally (e.g. Levis et al., 2012; Hudiburg et al., 2013; Raczka et al., 2016; Duarte et al., 2017). We do not seek to extend here these crucial evaluations of CLM performance, but rather focus our attention on regional characteristics of the drought–control run differences in CLM simulations. This approach provides a framework for using forthcoming IDE observations to help evaluate model performance. It also mitigates the impact of known CLM biases, described in above references, as they should largely cancel out when CLM fluxes are subtracted from one another.

We used the satellite phenology formulation of CLM4 for several reasons. First, this separates the GPP impacts of reduced precipitation from the greenness-increasing GPP impacts of CO_2 fertilization (Mankin et al., 2017). CLM4SP reports how CLM4 predicts drought should impact GPP per unit LAI. This per-unit-LAI result is useful both for examining a piece of future GPP responses to drought as well as interpreting IDE field observations in the present day, before the onset of late 21st century emissions-driven carbon fertilization. Though the prognostic carbon and nitrogen cycle formulations of CLM4 provide more parameters and simulate more processes, it does not necessarily follow that these simulations are more accurate. For example, two recent studies considered CLM simulations of LAI at two different evergreen needleleaf (ENF) sites in the Western USA, and demonstrated that in the absence of site-specific parameter estimations, CLM4.5 underestimated ENF LAI in Washington, USA (Duarte et al., 2017) and overestimated ENF LAI in Colorado, USA (Raczka et al., 2016). Our global simulation necessarily uses global (that is, non-site-specific) parameters. Using CLM4SP forces the model with realistic LAI and avoids the uncertainties of prognostic LAI.

We drove the control simulation with the “standard” forcing data for CLM4SP offline mode (section 17 of Oleson et al., 2010), which uses precipitation, solar radiation, temperature, wind, humidity, and pressure for the years 1972–2004 from Qian et al. (2006). The forcing data are on a global 2.0 by 2.0 degree grid at 6-hourly (precipitation, solar radiation) or 3-hourly (temperature, wind, humidity, pressure)

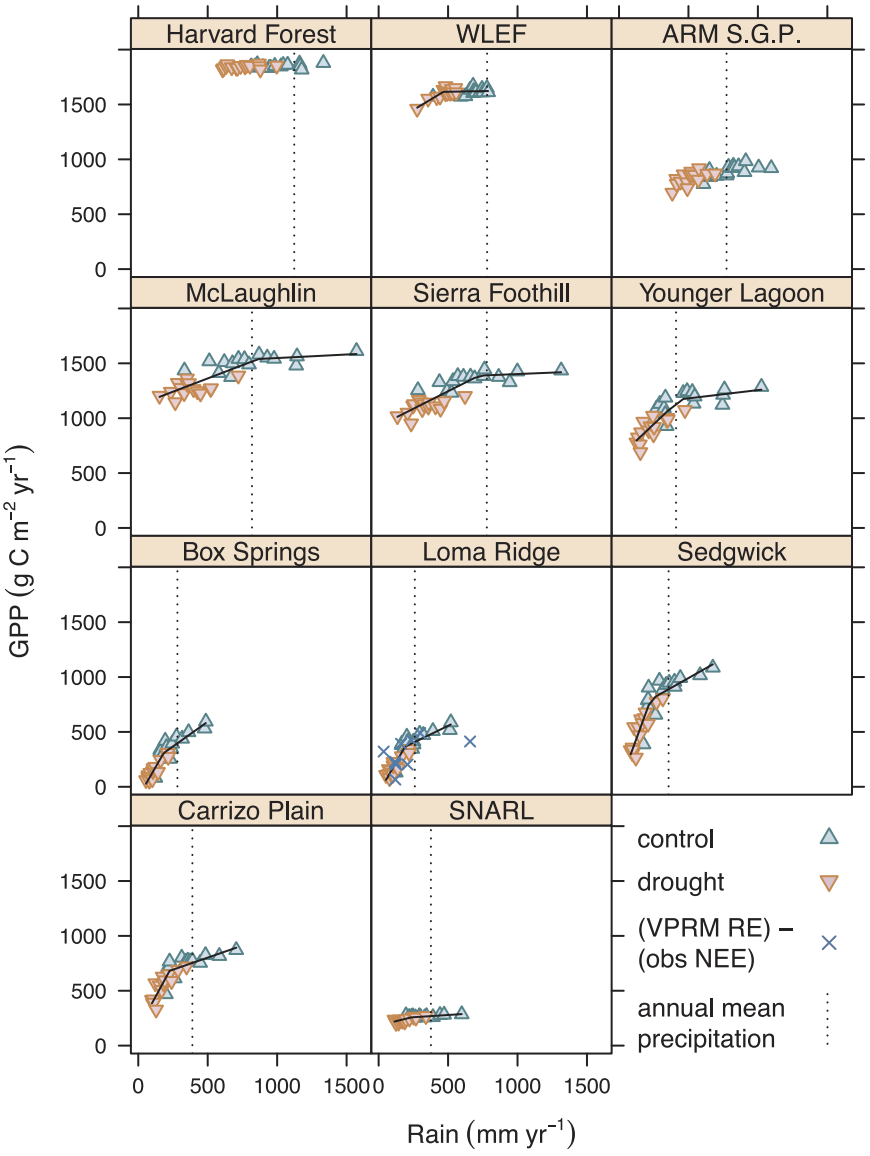

Fig. 2. Site-level empirical slope fits for modeled GPP–precipitation curves. Site locations are in Table 1 and Fig. 1b. AIC (Akaike, 1976) chose the two-slope fit (black lines) over a one-slope linear fit at all California sites demonstrating that CLM-simulated California GPP decreases more per unit decline in precipitation in drier conditions than in wetter conditions. Absence of a black line indicates that a one-slope linear best fit the data. Blue "X" markers on the Loma Ridge panel show GPP estimated by subtracting eddy covariance net ecosystem exchange (NEE) observations from Vegetation Photosynthesis and Respiration Model (VPRM) respiration (RE) as described in Section 2. Loma Ridge is the only one of the California sites that collects eddy covariance observations. (For interpretation of the references to color in this figure legend, the reader is referred to the web version of this article.)

temporal resolution.

Our experimental simulation is forced by precipitation we derived from the Qian et al. (2006) precipitation by reducing the magnitudes of all precipitation events according to the IDE experimental protocol. We calculated annual total precipitation within each grid cell for all years in the Qian et al. (2006) dataset (1948–2004), and within each grid cell calculated the 1st and 50th percentile of these annual precipitation totals. The 1st percentile approximates the one-in-one-hundred-year drought, while the 50th percentile approximates the 20th century long-term average precipitation. We calculated a reduction fraction for each grid cell as (1st percentile) divided by (50th percentile). We then multiplied each grid cell's 6-hourly precipitation time series by this grid cell reduction fraction to create a forcing dataset for the experimental run. The experimental run used unaltered (Qian et al., 2006) solar radiation, temperature, wind, humidity, and pressure to be consistent with the IDE protocol.

We conducted a 50 model-year CLM4SP spinup run (Kluzek, 2013) using the 1972–2004 Qian et al. (2006) atmospheric forcing data. CLM4SP recycles the atmospheric driver data automatically, so the 50 model-year spinup was forced by 1972–2004 data followed by 1972–1990 data. We ran the experimental and control runs as "hybrid" CLM4SP runs (Kluzek, 2013) initialized with the final model state of the spinup run.

We tested two models of the precipitation–GPP relationship. A simple linear regression describes a GPP–precipitation relationship with a single unchanging slope. Watts and Bacon (1974) presented a hyperbola that fits "two-regime straight-line data": data characterized by two straight lines on either side of a join point. The Watts and Bacon (1974) hyperbola, defined by five parameters, is a two-slope curve with arbitrary join point and slopes. Within every CLM grid cell we calculated linear fits using lm() from the R language and platform for statistical computing (R Core Team, 2017), and we estimated the Watts and Bacon (1974) slopes and join point using the DEoptim package in R (Ardia and Mullen, 2009). We used AIC (Akaike, 1976) to determine whether the one-slope linear or two-slope hyperbolic model best fit the CLM precipitation–GPP data. AIC provides a quantitative method to balance goodness of fit against parsimony when fitting a model to data.

Loma Ridge Global Change Experiment (Table 1) has made eddy covariance net ecosystem exchange (NEE) observations since 2007. Hilton et al. (2013) optimized site-specific parameter values for the Vegetation Photosynthesis Respiration Model (VPRM, Mahadevan et al., 2008) to these observations. We estimated Loma Ridge GPP independently from CLM by adding VPRM ecosystem respiration to eddy covariance-observed NEE. Loma Ridge is the only one of our eight California sites (Table 1) with co-located eddy covariance flux observations. As noted above, CLM has been compared extensively with

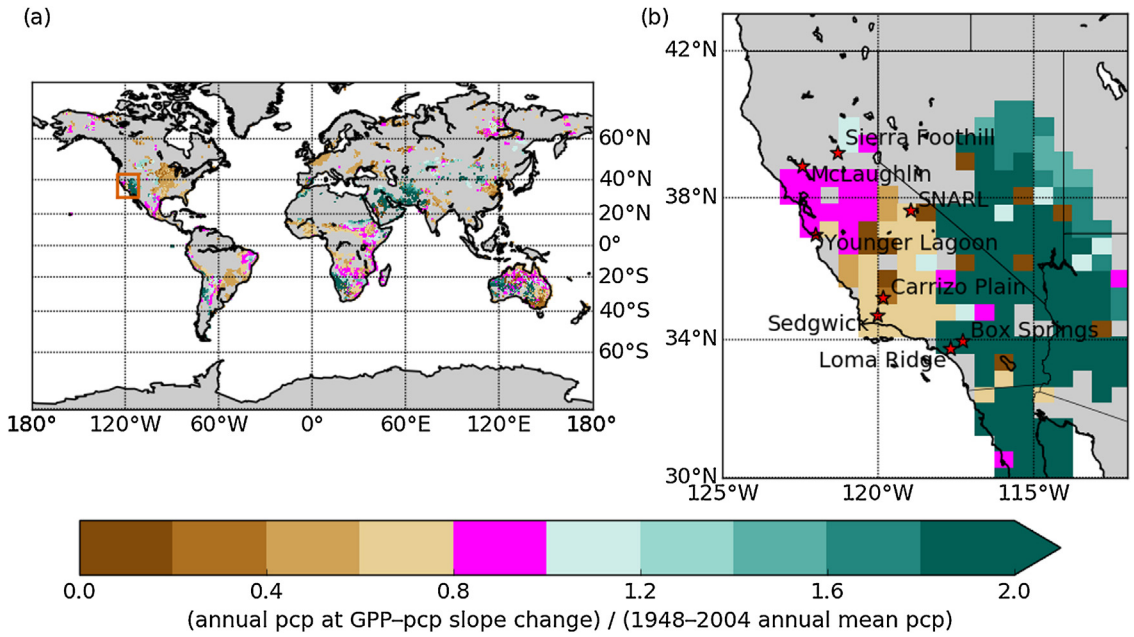

Fig. 3. Long-term mean annual precipitation (pcp) (Qian et al., 2006) versus the empirically fit transition point in the modeled GPP–pcp relationship. At colored points AIC (Akaike, 1976) preferred the two-regime straight-line fit (black lines) over a linear fit. At uncolored points GPP–pcp did not show a significant slope transition. Points in magenta show a ratio between 0.8 and 1.0, indicating that the long-term mean pcp is slightly wetter than the GPP-pcp inflection point. This suggests that a small decrease in pcp at these locations could produce a larger decline in GPP than previous behavior might indicate. (For interpretation of the references to color in this figure legend, the reader is referred to the web version of this article.)

eddy covariance flux observations, and we do not seek to extend these important analyses here. We do consider the Loma Ridge GPP estimates a useful reality check that CLM's simulations are plausible and useful for our purposes, and therefore report these observations along with CLM results.

3. Results

3.1. GPP–Precipitation slope transitions

Fig. 2 compares annual total GPP against annual total rainfall for the 15-year CLM control run and 15-year CLM drought run across the UCNRS sites. We quantitatively compared two descriptions of the GPP–precipitation curves in Fig. 2 (see Section 2). AIC chose the two–slope regime over the linear fit for all eight California sites (Fig. 1b). The overlaid black curves in Fig. 2 show these two-slope fits. The slope transition point occurs at 500–750 mm annual precipitation for the three wetter northerly sites (McLaughlin, Sierra Foothill, and Younger Lagoon), but at 250–300 mm annual precipitation for the drier southerly sites (Box Springs, Loma Ridge, and Sedgwick). The larger difference between mean annual precipitation and the slope transition point indicates the drier sites are resilient to larger precipitation reductions.

Fig. 3 generalizes Fig. 2 in space by showing the ratio of precipitation at the point of slope transition (see Section 2) to observed annual mean precipitation (calculated from 1948 to 2004 observations). Land grid cells plotted in gray are locations where AIC concluded a single-slope linear fit best fit the simulated GPP–precipitation relationship. Grid cells plotted in brown, green, or magenta are locations where AIC chose the two-slope GPP–precipitation curve as the best fit for the simulations. Grid cells plotted in shades of brown are locations where long-term mean precipitation is wetter than the slope transition point; that is, a drought could result in a switch to a different GPP–precipitation slope. Magenta grid cells are locations where the 1948 to 2004 mean observed precipitation is between 100% and 125% of the slope transition points. Long-term mean precipitation positions these points closer than others to entering a new GPP–precipitation slope as a result of a drought. In other words, a small decrease in precipitation at these locations could produce a larger decline in GPP than previous behavior might indicate. Much of Northern California, sizable portions of sub-Saharan Africa and Australia, and parts of the Amazon basin and Siberia are in this category.

3.2. Drought-induced annual cycle changes

Fig. 4 shows the modeled annual mean cycle for GPP at daily resolution for several sites in the coterminous USA.

The relatively mesic sites Harvard Forest (Massachusetts, USA) and WLEF (Wisconsin, USA) exhibit little decline in GPP even during one-in-100-year drought simulations. Moving from the relatively wet and humid eastern North America sites toward the more arid west, ARM S. Great Plains (Oklahoma, USA) exhibits a summer and autumn decline in GPP in the drought relative to the control runs. Northern California sites Sierra Foothill, McLaughlin, and Younger Lagoon show lower peak GPP magnitude, an earlier peak in the annual cycle, and annual total GPP reduction of 15% to 20% for drought relative to control simulations. These effects become even more pronounced at Southern California sites Box Springs, Loma Ridge, Sedgwick, and Carrizo Plain, with GPP reduction approaching 50% relative to control simulations.

Fig. 5 shows the annual cycle for transpiration beta factor (β_t) at daily resolution. β_t is an attenuation factor ranging from 0.0 to 1.0 employed within CLM that reduces simulated GPP according to soil moisture stress (Oleson et al., 2010). During the drought simulations the Southern California sites often experience near total reduction of GPP because of soil water stress, with β_t near zero at Box Springs and Loma Ridge for several months of the year during drought simulations. For the control simulations (driven by 1972–1987 observed precipitation), the β_t 95% confidence interval at these sites never dips below 0.10. This indicates that complete downregulation of GPP never occurred in the control simulations, even though their driving precipitation included the severe drought of 1976–1977 (Cal. Dept. of Water Resources, 1983).

Fig. 6, Fig. 7, and Fig. 8 generalize these analyses to the mean annual cycle decline in maximum GPP magnitude, percent decline, and

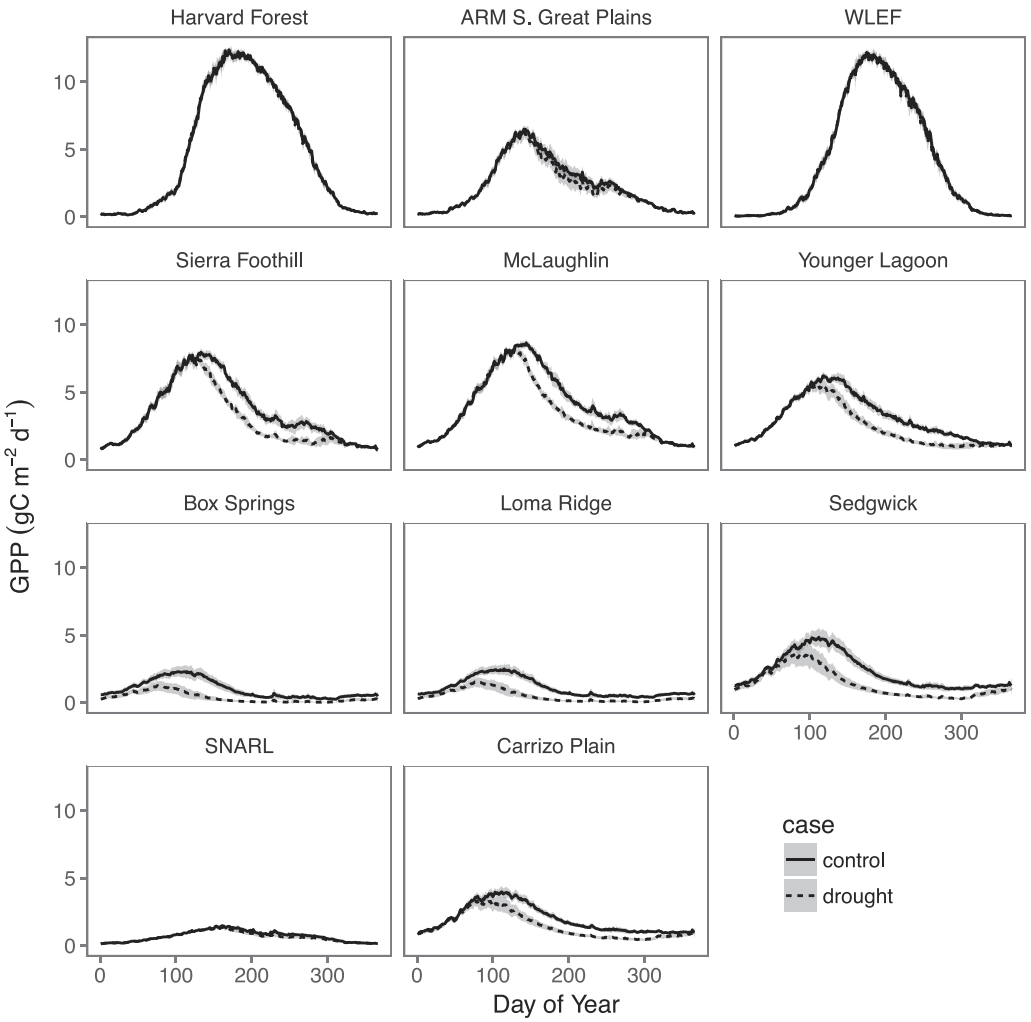

Fig. 4. Mean annual cycle (solid and dashed lines) and 95% confidence intervals (gray envelopes) in CLM GPP at selected U.S. analysis sites (site locations in Fig. 1b and Table 1). The means are calculated over the 15-year simulations (see Section 2).

shift in the day of year of annual maximum GPP, respectively, for each CLM grid cell. Virtually every location shows some decline in annual maximum GPP during severe drought, with the southwestern USA, much of sub-Saharan Africa, Eastern Brazil, and Australia showing the largest GPP declines in excess of 40% (Figs. 6 and 7). These same regions, with the addition of western South America, show a pronounced shift in the timing of the annual cycle (Fig. 8), with the annual maximum GPP occurring several weeks to more than a month earlier in the growing season for the drought scenario.

4. Discussion

GPP–climate feedback uncertainties are responsible for much of the overall spread in global climate predictions (Friedlingstein et al., 2014; Ciais et al., 2013), and a substantial portion of these feedback uncertainties originate in the effects of water availability on GPP (Lei et al., 2014). A change in the slope of GPP versus precipitation identifies a precipitation amount at which the GPP response to a given precipitation change enters a different phase. Examining the CLM precipitation–GPP curves (Figs. 2 and 3) for a discrete change in slope tests the hypothesis that plants in more arid and drought-prone areas (e.g. Southern California) should display a greater resilience to severe drought conditions than plants in more temperate hydrologic climes (e.g. Northern California). The six sites where a two-slope regime best fit the GPP–pcp data (Fig. 2) show a steeper drop in GPP per unit precipitation decrease at low precipitation levels than at higher levels. This demonstrates that GPP sensitivity to drought increases with increasing drought severity, but also that GPP rebounds more quickly from a severe drought than from a milder drought per unit of precipitation increase.

All of the eight sites examined in California exhibited a significant slope change in the GPP–precipitation curve. This occurred between 500 and 750 mm annual precipitation for Northern California, and around 300 mm annual precipitation for Southern California. This demonstrates a steeper decline in GPP per unit precipitation reduction at drier sites, but also a more responsive increase per unit precipitation following a return to wetter conditions.

A large section of Northern California – and many other areas around the world – featured mean 1948–2004 annual precipitation values between 100 and 125 percent of the GPP–precipitation slope change (magenta areas in Fig. 3). This suggests that these locations may see a more drastic decline in GPP during drought conditions than past observations might suggest, at least under the conditions used in the present study. Also, although Northern California typically sees more precipitation and photosynthetic productivity relative to Southern California, Northern California also appears to have a reduced margin between 20th century norms and the transition point to steeper GPP reduction per unit precipitation decrease (Fig. 3, right panel).

Transpiration beta factor (β_t) parameterizes the effect of drought stress on GPP, and does not attempt to describe plant hydraulic stress mechanistically. This is a known shortcoming of CLM version 4.5 (Trugman et al., 2018), and β_t has been replaced with a mechanistic

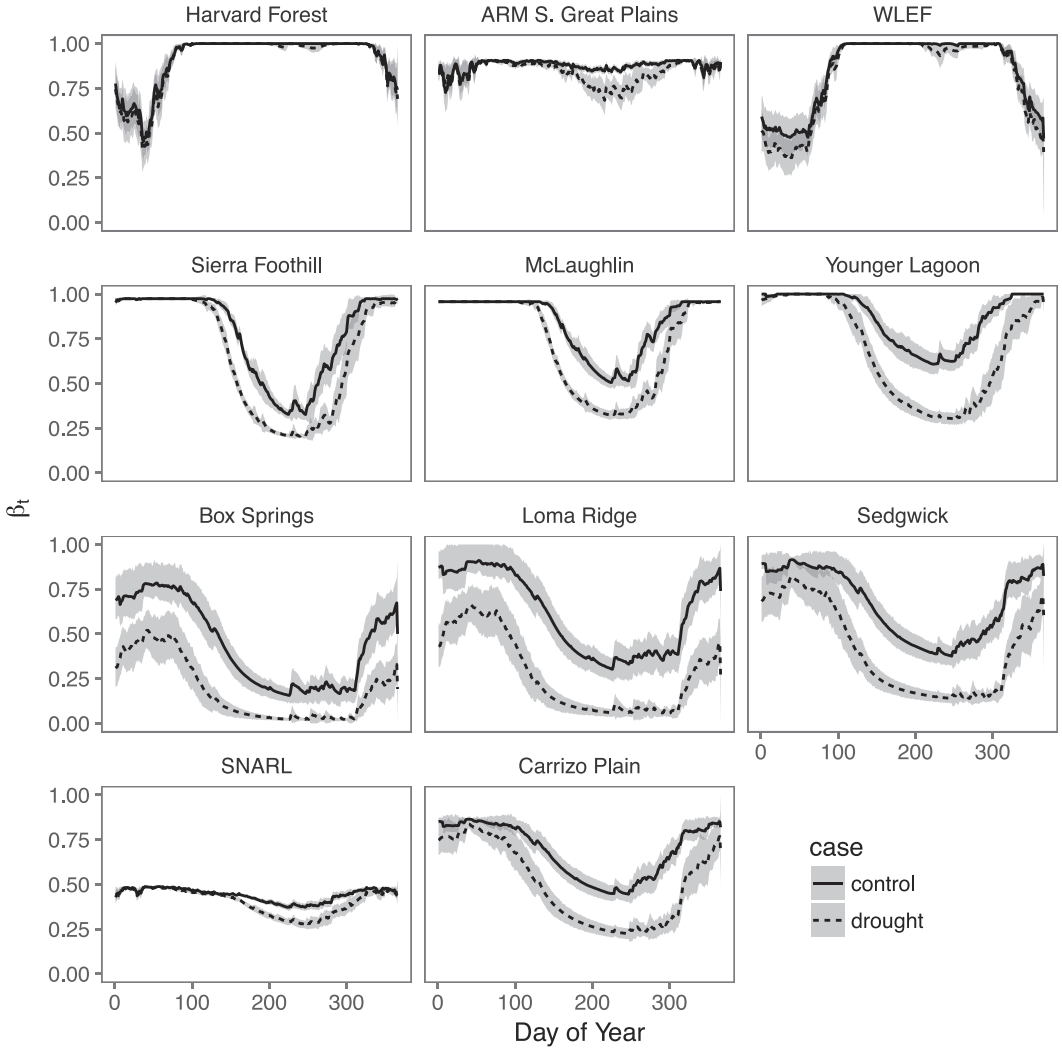

Fig. 5. Mean annual cycle (solid and dashed lines) and 95% confidence intervals (gray envelopes) in CLM transpiration beta factor (β_t) parameter at selected U.S. analysis sites (site locations in Fig. 1b and Table 1). Within CLM (β_t) varies between 0.0 and 1.0 to attenuate photosynthesis (Oleson et al., 2010) in response to soil water shortage.

description of hydraulic stress in CLM version 5.0 (Lawrence et al., 2018). CLM 5.0 was not yet released when our work was performed. Despite this non-mechanistic treatment of hydraulic stress in CLM4SP, the difference in β_t from our control run to our drought-forced run exhibits regional coherence in both Northern and Southern California, and is consistent across sites in those regions. This suggests that CLM sees differences in hydraulic stress response to severe drought between these regions.

The CLM-diagnosed transpiration beta factor suggests that vegetation in Northern California does not experience wet season limitation of GPP from low soil moisture, even during many years of consecutive severe drought. Severe drought extends the dry season period of soil moisture constraints on GPP to earlier in the spring and later into the autumn relative to non-drought conditions. Indeed, timing of soil moisture availability may be more important than precipitation amount for GPP in California grasslands (Xu and Baldocchi, 2004). Similarly, the timing of the onset of the dry season is key for productivity of Mediterranean forest ecosystems (Maselli et al., 2014).

Southern California sites face GPP limitation from low soil moisture at virtually all times, and may see near complete reduction of GPP owing to soil moisture stress during severe drought. This condition never arose during control simulations driven by observed late 20th century climate.

Our results suggest that vegetation processes related to GPP may be impacted differently by a 1-in-100 year drought in Northern versus Southern California, with Southern California's annual GPP experiencing a relatively larger magnitude reduction and a more pronounced change in its seasonal cycle timing. Sizable parts of sub-Saharan Africa, Australia, and the Amazon responded to drought similarly to Southern California.

The results reported here are not meant to comprehensively forecast future ecosystem responses to severe drought, but rather to provide context for interpreting field experiments and remote sensing products. The four following caveats should guide interpretation of the results reported here. First, CLM grid cells are essentially independent of one another, with inter-gridcell transport of above- and below-ground water, energy, and mass handled by other components of CESM that are beyond the scope of this study and therefore were not activated. The results we report simulate the response of each CLM grid cell to a severe drought independent of interactions with other gridcells except as prescribed by the static atmospheric driver data.

Second, our CLM4SP simulations examine the plant response to severe drought while holding leaf area index (LAI) constant. This is a useful accompaniment to remote sensing drought impact measures because drought-driven phenology changes can be difficult to disentangle from longer-term changes in an ecosystem (Assal et al., 2016). Moreover, CLM prognostic LAI is known to over-estimate LAI at some sites while under-estimating at similar sites in the absence of site-

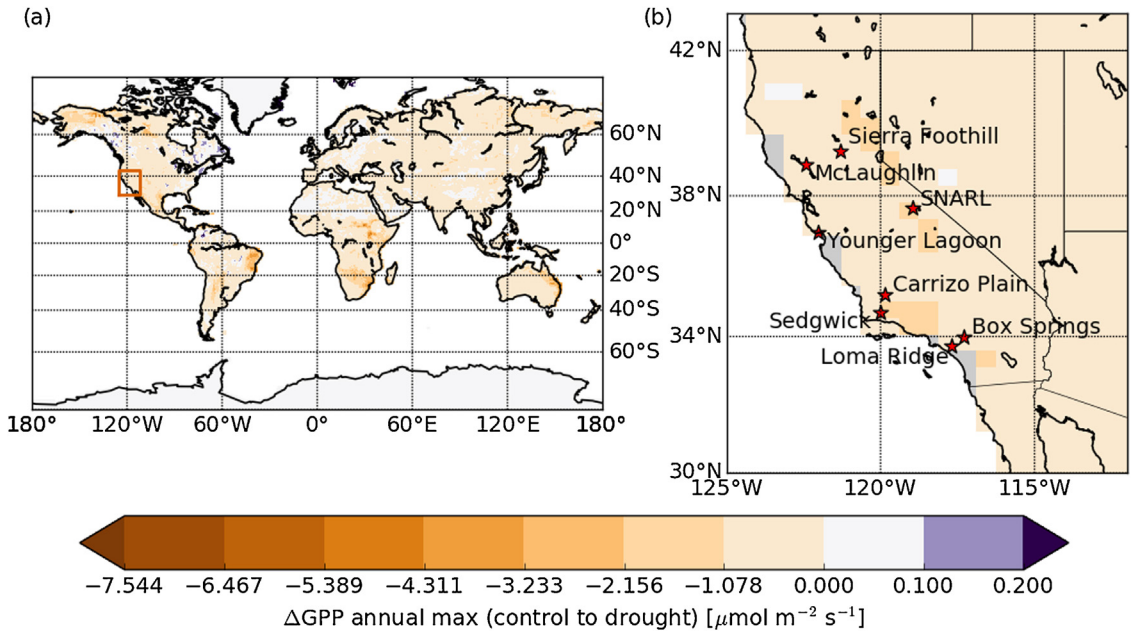

Fig. 6. Absolute decline in mean annual maximum CLM GPP, CLM control runs to CLM drought runs (drought minus control). Grey land areas denote areas masked to water on the CLM 0.47 by 0.63 degree grid. (For interpretation of colors in this figure legend, the reader is referred to the web version of this article.)

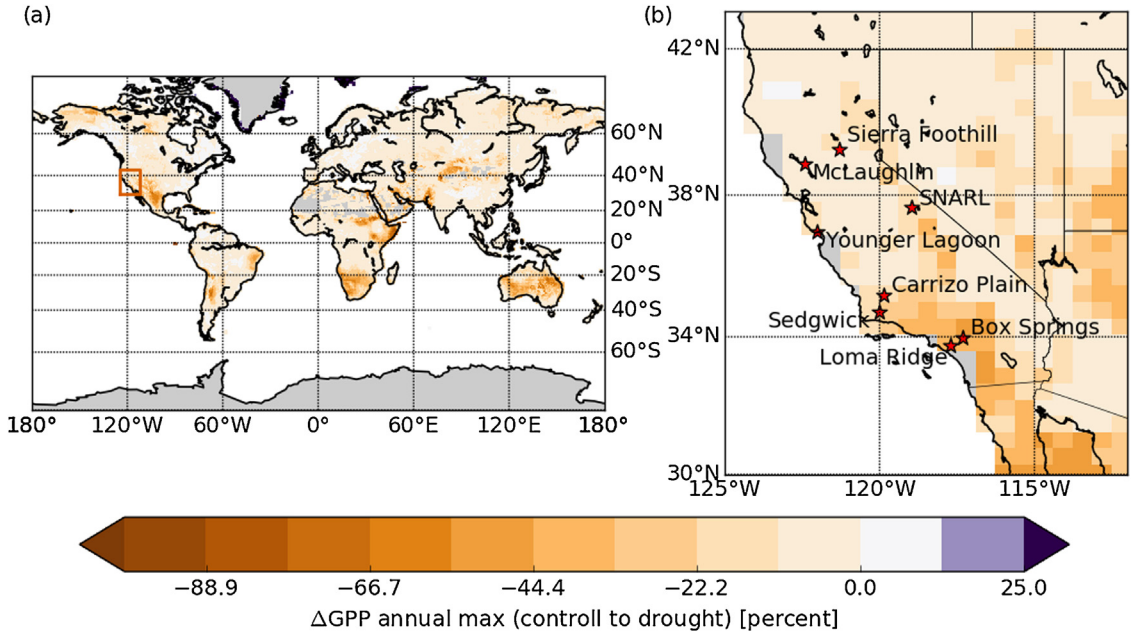

Fig. 7. Percent decline in mean annual maximum CLM GPP, CLM control runs to CLM drought runs. Grey land areas denote areas masked to water on the CLM 0.47 by 0.63 degree grid. (For interpretation of colors in this figure legend, the reader is referred to the web version of this article.)

specific parameterization (Duarte et al., 2017; Raczka et al., 2016). Leaf area changes are a primary response to drought (Wellstein et al., 2017); this is one of reasons that our results are not a comprehensive prediction of drought response. They are instead a measure of CLM's expectation of drought impacts *per unit LAI*.

Third, all CLM runs in the present study were driven by observed atmospheric CO_2 concentrations from the year 2000 (compset I_2000). This choice simulates the ambient CO_2 conditions prescribed by the IDE experimental protocol so that the CLM results can aid interpretation of IDE results and IDE results may inform future CLM work. Constructing model runs this way isolates them from the carbon dioxide fertilization effects that many models predict will accompany future drought realizations.

Fourth, by its nature the IDE cannot – and our model experiment therefore does not – simulate increased atmospheric demand for water due to warmer temperatures and drought-driven lower humidity. This is another reason that our results are more useful for interpreting upcoming field experiments than comprehensively forecasting future real-world conditions. The regional coherence of GPP–precipitation slope changes (Fig. 3) can, however, provide guidance for extrapolating IDE observations in space. For example, Fig. 3b identifies a subset of Northern California that could be more likely to experience GPP reduction from reduced precipitation in excess of what a 20th century observed GPP–precipitation regression would predict. Were IDE observations to confirm this, the spatial extent of the affected region might not be entirely obvious from purely remote-sensing based land

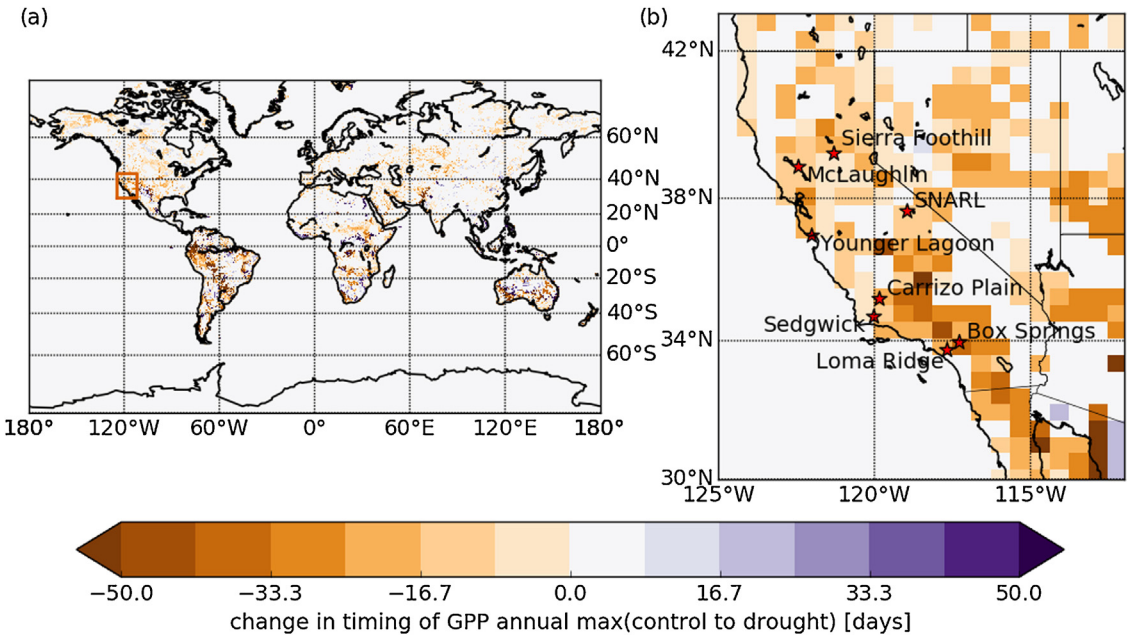

Fig. 8. Shift in day of year of mean annual maximum CLM GPP, CLM control runs to CLM drought runs. (For interpretation of colors in this figure legend, the reader is referred to the web version of this article.)

surface classifications such as plant functional types.

Future work could more thoroughly investigate the ability of CLM in our configuration to produce GPP estimations that match flux observation-informed GPP estimates at more field sites. This work, beyond the scope of the present study, could support or discourage interpreting our results to predict future real-world conditions.

In any interpretation, our results demonstrate the highly regional nature of ecosystem drought responses. Key sectors in California and worldwide – water management and agricultural production – as well as land management for biodiversity, wildland fire risk, and forest health, should plan for regionally-specific sensitivity to extreme drought.

Code availability

Source code and documentation for all components of the CESM version 1.2 is available from http://www.cesm.ucar.edu/models/cesm1.2/ (accessed 18 November 2018).

Supporting code for analyses described here is archived at https://github.com/Timothy-W-Hilton/CLM_IDE_analyses.

Competing interests

None.

Acknowledgments

Yaqiong Lu of The National Center for Atmospheric Research provided support and consultation for setting up our CLM experiments. This work was funded by the University of California's Institute for the Study of Ecological & Evolutionary Climate Impacts (ISEECI). The CESM project is supported by the National Science Foundation and the Office of Science (BER) of the U.S. Department of Energy. The authors acknowledge the work of UCNRS directors G. Dayton (Younger Lagoon Reserve), P. Aigner and C. Koehler (McLaughlin Reserve), K. McCurdy (Sedgwick Reserve) in supporting IDE fieldwork. This research used resources of the National Energy Research Scientific Computing Center, which is supported by the Office of Science (BER) of the U.S. Department of Energy under Contract No. DE-AC02-05CH11231. Data pre- and post-processing were performed using SciPy (Jones et al., 2001), Matplotlib (Hunter, 2007), and Pandas (McKinney, 2010) and the Differential Evolution package (Ardia and Mullen, 2009) for the R language and platform for statistical computing (R Core Team, 2017).

References

Akaike, H., 1976. An information criterion (AIC). Math. Sci. 14 (153), 5–9.

Anderegg, W.R.L., Klein, T., Bartlett, M., Sack, L., Pellegrini, A.F.A., Choat, B., Jansen, S., 2016. Meta-analysis reveals that hydraulic traits explain cross-species patterns of drought-induced tree mortality across the globe. Proc. Natl. Acad. Sci. 113 (18), 5024–5029. https://doi.org/10.1073/pnas.1525678113.

Ardia, D., Mullen, K., 2009. DEoptim: Differential Evolution Optimization in R. R package version 2.0-1. http://CRAN.R-project.org/package=DEoptim, last accessed 1 June 2012.

Assal, T.J., Anderson, P.J., Sibold, J., 2016. Spatial and temporal trends of drought effects in a heterogeneous semi-arid forest ecosystem. Forest Ecol. Manag. 365, 137–151. https://doi.org/10.1016/j.foreco.2016.01.017.

Bonan, G.B., Lawrence, P.J., Oleson, K.W., Levis, S., Jung, M., Reichstein, M., Lawrence, D.M., Swenson, S.C., 2011. Improving canopy processes in the Community Land Model version 4 (CLM4) using global flux fields empirically inferred from FLUXNET data. J. Geophys. Res. Biogeosci. 116 (G2). https://doi.org/10.1029/2010JG001593. G02,014.

Buck-Diaz, J., Evens, J., 2011. Carrizo Plain National Monument vegetation classification and mapping project, Draft report prepared for the Bureau of Land Management. California Native Plant Society, Sacramento, CA , accessed 21 June 2017. http://www.cnps.org/cnps/vegetation/pdf/carrizo-vegetation_rpt2011.pdf.

Cal. Dept. of Water Resources, 1983. Summary of water conditions, DWR Bulletin 120. http://cdec.water.ca.gov/snow/bulletin120/5, accessed 31 May 2017.

Cal. Dept. of Water Resources, 2017. Summary of water conditions, DWR Bulletin 120. http://cdec.water.ca.gov/snow/bulletin120/, accessed 22 May 2017.

CESM Software Engineering Group (CSEG), 2013. CESM1.2 Release Series Users Guide. NCAR, National Center for Atmospheric Research, Boulder, CO, USA , accessed 25 August 2016. http://www.cesm.ucar.edu/models/cesm1.2/.

Cheng, L., Hoerling, M., AghaKouchak, A., Livneh, B., Quan, X.-W., Eischeid, J., 2016. How has human-induced climate change affected California drought risk? J. Clim. 29 (1), 111–120. https://doi.org/10.1175/JCLI-D-15-0260.1.

Ciais, P., Sabine, C., Bala, G., Bopp, L., Brovkin, V., Canadell, J., Chhabra, A., DeFries, R., Galloway, J., Heimann, M., Jones, C., Le Le Quéré, C., Myneni, R., Piao, S., Thornton, P., 2013. Carbon and Other Biogeochemical Cycles, book section 6. Cambridge University Press, Cambridge, United Kingdom and New York, NY, USA, pp. 465–570. https://doi.org/10.1017/CBO9781107415324.015.

Clark, J.S., Iverson, L., Woodall, C.W., Allen, C.D., Bell, D.M., Bragg, D.C., D'Amato, A.W., Davis, F.W., Hersh, M.H., Ibanez, I., Jackson, S.T., Matthews, S., Pederson, N., Peters, M., Schwartz, M.W., Waring, K.M., Zimmermann, N.E., 2016. The impacts of increasing drought on forest dynamics, structure, and biodiversity in the United States. Global Change Biol. 22 (7), 2329–2352. https://doi.org/10.1111/gcb.13160.

Collins, M., Knutti, R., Arblaster, J., Dufresne, J.-L., Fichefet, T., Friedlingstein, P., Gao, X., Gutowski, W., Johns, T., Krinner, G., Shongwe, M., Tebaldi, C., Weaver, A.,

Wehner, M., 2013. Long-term climate change: projections, commitments and irreversibility. In: Stocker, T., Qin, D., Plattner, G.-K., Tignor, M., Allen, S., Boschung, J., Nauels, A., Xia, Y., Bex, V., Midgley, P. (Eds.), Climate Change 2013: The Physical Science Basis. Contribution of Working Group I to the Fifth Assessment Report of the Intergovernmental Panel on Climate Change. Cambridge University Press, Cambridge, United Kingdom and New York, NY, USA, pp. 1029–1136. https://doi.org/10.1017/CBO9781107415324.024. (Chapter 12).

Cook, B.I., Ault, T.R., Smerdon, J.E., 2015. Unprecedented 21st century drought risk in the American Southwest and Central Plains. Sci. Adv. 1 (1). https://doi.org/10.1126/sciadv.1400082.

Dai, A., 2012. Increasing drought under global warming in observations and models. Nat. Clim. Change 3 (1), 52–58.

Davis, K., Bakwin, P.S., Yi, C., Berger, B., Zhao, C., Teclaw, R., Isebrands, J., 2003. The annual cycles of CO_2 and H_2O exchange over a northern mixed forest as observed from a very tall tower. Global Change Biol. 9 (9), 1278–1293.

Duarte, H.F., Raczka, B.M., Ricciuto, D.M., Lin, J.C., Koven, C.D., Thornton, P.E., Bowling, D.R., Lai, C.-T., Bible, K.J., Ehleringer, J.R., 2017. Evaluating the Community Land Model (CLM4.5) at a coniferous forest site in northwestern United States using flux and carbon-isotope measurements. Biogeosciences 14 (18), 4315–4340 copyright - Copyright Copernicus GmbH 2017; Last updated: 2018-03-20; SubjectsTermNotLitGenreText - United States-US.

Fauset, S., Baker, T.R., Lewis, S.L., Feldpausch, T.R., Affum-Baffoe, K., Foli, E.G., Hamer, K.C., Swaine, M.D., 2012. Drought-induced shifts in the floristic and functional composition of tropical forests in Ghana. Ecol. Lett. 15 (10), 1120–1129. https://doi.org/10.1111/j. 1461-0248.2012.01834.x.

Fischer, M.L., Billesbach, D.P., Berry, J.A., Riley, W.J., Torn, M.S., 2007. Spatiotemporal variations in growing season exchanges of CO_2, H_2O, and sensible heat in agricultural fields of the Southern Great Plains. Earth Interact. 11 (17), 1–21.

Friedlingstein, P., Meinshausen, M., Arora, V.K., Jones, C.D., Anav, A., Liddicoat, S.K., Knutti, R., 2014. Uncertainties in CMIP5 climate projections due to carbon cycle feedbacks. J. Clim. 27 (2), 511–526. https://doi.org/10.1175/JCLI-D-12-00579.1.

Griffin, D., Anchukaitis, K.J., 2014. How unusual is the 2012–2014 California drought? Geophys. Res. Lett. 41 (24), 9017–9023. https://doi.org/10.1002/2014GL062433, 2014GL062433.

Hilton, T.W., Davis, K.J., Keller, K., Urban, N.M., 2013. Improving North American terrestrial CO_2 flux diagnosis using spatial structure in land surface model residuals. Biogeosciences 10 (7), 4607–4625. https://doi.org/10.5194/bg-10-4607-2013.

Hilton, T.W., Davis, K.J., Keller, K., 2014. Evaluating terrestrial CO_2 flux diagnoses and uncertainties from a simple land surface model and its residuals. Biogeosciences 11 (2), 217–235. https://doi.org/10.5194/bg-11-217-2014.

Hogg, E., Brandt, J.P., Michaelian, M., 2008. Impacts of a regional drought on the productivity, dieback, and biomass of western Canadian aspen forests. Can. J. Forest Res. 38 (6), 1373–1384. https://doi.org/10.1139/X08-001.

Hudiburg, T.W., Law, B.E., Thornton, P.E., 2013. Evaluation and improvement of the Community Land Model (CLM4) in Oregon forests. Biogeosciences 10 (1), 453–470. https://doi.org/10.5194/bg-10-453-2013.

Hunter, J.D., 2007. Matplotlib: a 2D graphics environment. Comput. Sci. Eng. 9 (3), 90–95.

IPCC, 2013. Climate Change 2013: The Physical Science Basis. Contribution of Working Group I to the Fifth Assessment Report of the Intergovernmental Panel on Climate Change. Cambridge University Press, Cambridge, United Kingdom and New York, NY, USA. https://doi.org/10.1017/CBO9781107415324. 1535 pp.

Jones, E., Oliphant, T., Peterson, P., et al., 2001. SciPy: Open source scientific tools for Python. http://www.scipy.org/, last accessed 31 May 2017.

Kluzek, E., 2013. CESM Research Tools: CLM4.5 in CESM1.2.0 User's Guide Documentation. National Center for Atmospheric Research, Boulder, CO, USA , accessed 25 Aug 2016. http://www.cesm.ucar.edu/models/cesm1.2/clm/.

Knapp, A.K., Avolio, M.L., Beier, C., Carroll, C.J.W., Collins, S.L., Dukes, J.S., Fraser, L.H., Griffin-Nolan, R.J., Hoover, D.L., Jentsch, A., Loik, M.E., Phillips, R.P., Post, A.K., Sala, O.E., Slette, I.J., Yahdjian, L., Smith, M.D., 2017. Pushing precipitation to the extremes in distributed experiments: recommendations for simulating wet and dry years. Global Change Biol. 23 (5), 1774–1782. https://doi.org/10.1111/gcb.13504.

Lawrence, D., Fisher, R., Koven, C., Oleson, K., Swenson, S., Vertenstein, M., Andre, B., Bonan, G., Ghimire, B., van Kampenhout, L., Kennedy, D., Kluzek, E., Knox, R., Lawrence, P., Li, F., Li, H., Lombardozzi, D., Lu, Y., Perket, J., Riley, W., Sacks, W., Shi, M., Wieder, W., Xu, C., Ali, A., Badger, A., Bisht, G., Broxton, P., Brunke, M., Buzan, J., Clark, M., Craig, T., Dahlin, K., Drewniak, B., Emmons, L., Fisher, J., Flanner, M., Gentine, P., Lenaerts, J., Levis, S., Leung, L.R., Lipscomb, W., Pelletier, J., Ricciuto, D.M., Sanderson, B., Shuman, J., Slater, A., Subin, Z., Tang, J., Tawfik, A., Thomas, Q., Tilmes, S., Vitt, F., Zeng, X., 2018. Technical Description of version 5.0 of the Community Land Model (CLM). , accessed 16 November 2018. http://www.cesm.ucar.edu/models/cesm2/land/CLM50_Tech_Note.pdf.

Lawrence, D.M., Oleson, K.W., Flanner, M.G., Thornton, P.E., Swenson, S.C., Lawrence, P.J., Zeng, X., Yang, Z.-L., Levis, S., Sakaguchi, K., Bonan, G.B., Slater, A.G., 2011. Parameterization improvements and functional and structural advances in Version 4 of the Community Land Model. J. Adv. Model. Earth Syst. 3 (1). https://doi.org/10.1029/2011MS00045. M03,001.

Lei, H., Huang, M., Leung, L.R., Yang, D., Shi, X., Mao, J., Hayes, D.J., Schwalm, C.R., Wei, Y., Liu, S., 2014. Sensitivity of global terrestrial gross primary production to hydrologic states simulated by the Community Land Model using two runoff parameterizations. J. Adv. Model. Earth Syst. 6 (3), 658–679. https://doi.org/10.1002/2013MS000252.

Levis, S., Bonan, G.B., Kluzek, E., Thornton, P.E., Jones, A., Sacks, W.J., Kucharik, C.J., 2012. Interactive crop management in the Community Earth System Model (CESM1): seasonal influences on land-atmosphere fluxes. J. Clim. 25 (14), 4839–4859. https://doi.org/10.1175/JCLI-D-11-00446.1.

Liu, S., Zhuang, Q., Chen, M., Gu, L., 2016. Quantifying spatially and temporally explicit CO_2 fertilization effects on global terrestrial ecosystem carbon dynamics. Ecosphere 7 (7). https://doi.org/10.1002/ecs2.1391. e01,391–n/a.

Mahadevan, P., Wofsy, S., Matross, D., Xiao, X., Dunn, A., Lin, J., Gerbig, C., Munger, J., Chow, V., Gottlieb, E., 2008. A satellite-based biosphere parameterization for net ecosystem CO_2 exchange: vegetation photosynthesis and respiration model (VPRM). Global Biogeochem. Cycles 22, GB2005. https://doi.org/10.1029/2006GB002735.

Mankin, J.S., Smerdon, J.E., Cook, B.I., Williams, A.P., Seager, R., 2017. The curious case of projected twenty-first-century drying but greening in the American West. J. Clim. 30 (21), 8689–8710. https://doi.org/10.1175/JCLI-D-17-0213.1.

Maselli, F., Cherubini, P., Chiesi, M., Gilabert, M.A., Lombardi, F., Moreno, A., Teobaldelli, M., Tognetti, R., 2014. Start of the dry season as a main determinant of inter-annual Mediterranean forest production variations. Agric. Forest Meteorol. 194, 197–206. https://doi.org/10.1016/j.agrformet.2014.04.006.

McDowell, N.G., Williams, A., Xu, C., Pockman, W., Dickman, L., Sevanto, S., Pangle, R., Limousin, J., Plaut, J., Mackay, D., et al., 2015. Multi-scale predictions of massive conifer mortality due to chronic temperature rise. Nat. Clim. Change 6 (1), 295–300.

McKinney, W., 2010. Data structures for statistical computing in python. In: van der Walt, S., Millman, J. (Eds.), Proceedings of the 9th Python in Science Conference, pp. 51–56.

Millikin, C.S., Bledsoe, C.S., 1999. Biomass and distribution of fine and coarse roots from blue oak (*Quercus douglasii*) trees in the northern Sierra Nevada foothills of California. Plant Soil 214 (1), 27–38. https://doi.org/10.1023/A:1004653932675.

Nelson, M.B., Berlemont, R., Martiny, A.C., Martiny, J.B., 2015. Nitrogen cycling potential of a grassland litter microbial community. Appl. Environ. Microbiol. 81 (20), 7012–7022. https://doi.org/10.1128/AEM.02222-15.

NOAA National Centers for Environmental information, 2017. Climate at a Glance: U.S. Time Series, Precipitation, published May 2017. Retrieved on May 26, 2017. http://www.ncdc.noaa.gov/cag/.

Ogle, K., Barber, J.J., Barron-Gafford, G.A., Bentley, L.P., Young, J.M., Huxman, T.E., Loik, M.E., Tissue, D.T., 2015. Quantifying ecological memory in plant and ecosystem processes. Ecol. Lett. 18 (3), 221–235. https://doi.org/10.1111/ele.12399.

Oleson, K.W., Lawrence, D.M., Bonnan, G., Flanner, M.G., Kluzek, E.P.J., Levis, S., Swenson, S.C., Thornton, E., Feddema, J., Heald, C.L., Lamarque, J.-F., yue Niu, G., Qian, T., Running, S., Sakaguchi, K., Yang, L., Zeng, X., Zeng, X., 2010. Technical Description of version 4.0 of the Community Land Model (CLM). https://doi.org/10.5065/D6FB50WZ.

Prein, A.F., Holland, G.J., Rasmussen, R.M., Clark, M.P., Tye, M.R., 2016. Running dry: the U.S. Southwest's drift into a drier climate state. Geophys. Res. Lett. 43 (3), 1272–1279. https://doi.org/10.1002/2015GL066727, 2015GL066727.

Prudhomme, C., Giuntoli, I., Robinson, E.L., Clark, D.B., Arnell, N.W., Dankers, R., Fekete, B.M., Franssen, W., Gerten, D., Gosling, S.N., Hagemann, S., Hannah, D.M., Kim, H., Masaki, Y., Satoh, Y., Stacke, T., Wada, Y., Wisser, D., 2014. Hydrological droughts in the 21st century, hotspots and uncertainties from a global multimodel ensemble experiment. Proc. Natl. Acad. Sci. 111 (9), 3262–3267. https://doi.org/10.1073/pnas.1222473110.

Qian, T., Dai, A., Trenberth, K.E., Oleson, K.W., 2006. Simulation of global land surface conditions from 1948 to 2004. Part I: Forcing data and evaluations. J. Hydrometeorol. 7 (5), 953–975. https://doi.org/10.1175/JHM540.1.

R Core Team, 2017. R: A Language and Environment for Statistical Computing. R Foundation for Statistical Computing, Vienna, Austria last accessed 31 May 2017. ISBN 3-900051-07-0.

Raczka, B., Duarte, H.F., Koven, C.D., Ricciuto, D., Thornton, P.E., Lin, J.C., Bowling, D.R., 2016. An observational constraint on stomatal function in forests: evaluating coupled carbon and water vapor exchange with carbon isotopes in the Community Land Model (CLM4.5). Biogeosciences 13 (18), 5183–5204. https://doi.org/10.5194/bg-13-5183-2016.

Reed, C.C., Loik, M.E., 2016. Water relations and photosynthesis along an elevation gradient for *Artemisia tridentata* during an historic drought. Oecologia 181 (1), 65–76. https://doi.org/10.1007/s00442-015-3528-7.

Reed, L., Hatch, M., Valenta, K., Holl, K., 2011. Reference site characterization and restoration goals for northern coastal scrub and seasonal wetlands at Younger Lagoon Reserve. Report for the California Coastal Commission. http://ucsantacruz.ucnrs.org/wp-content/uploads/documents/Reed%20et%20al%202011-Coastal%20freshwater%20wetland%20and%20coastal%20scrub%20reference%20conditions.pdf, accessed 15 June 2017.

Reichstein, M., Bahn, M., Ciais, P., Frank, D., Mahecha, M.D., Seneviratne, S.I., Zscheischler, J., Beer, C., Buchmann, N., Frank, D.C., Papale, D., Rammig, A., Smith, P., Thonicke, K., van der Velde, M., Vicca, S., Walz, A., Wattenbach, M., 2013. Climate extremes and the carbon cycle. Nature 500 (7462), 287–295 perspectives.

Robeson, S.M., 2015. Revisiting the recent California drought as an extreme value. Geophys. Res. Lett. 42 (16), 6771–6779. https://doi.org/10.1002/2015GL064593, 2015GL064593.

Schaefer, K., Schwalm, C., Williams, C., Arain, A., Barr, A., Chen, J., Davis, K., Dimitrov, D., Golaz, N., Hilton, T., Hollinger, D., Humphreys, E., Poulter, B., Raczka, B., Richardson, A., Sahoo, A., Thornton, P., Vargas, R., Verbeeck, H., Anderson, R., Baker, I., Baldocchi, D., Black, T.A., Bolstad, P., Chen, J., Curtis, P., Desai, A., Dietze, M., Dragoni, D., Flanagan, L., Grant, R., Gu, L., Katul, G., Kucharik, C., Law, B., Liu, S., Lokipitiya, E., Margolis, H., Matamala, R., McCaughey, H., Monson, R., Munger, J.W., Oechel, W., Peng, C., Price, D., Ricciuto, D., Riley, B., Roulet, N., Tian, H., Tonitto, C., Torn, M., Verma, S., Weng, E., 2012. A model-data comparison of gross primary productivity. J. Geophys. Res. 117https://doi.org/10.1029/2012JG001960. G03,010.

Schimel, D., Stephens, B.B., Fisher, J.B., 2015. Effect of increasing CO_2 on the terrestrial carbon cycle. Proc. Natl. Acad. Sci. 112 (2), 436–441. https://doi.org/10.1073/pnas.1407302112.

Seager, R., Vecchi, G.A., 2010. Greenhouse warming and the 21st century hydroclimate of southwestern North America. Proc. Natl. Acad. Sci. 107 (50), 21277–21282. https://doi.org/10.1073/pnas.0910856107.

Seager, R., Ting, M., Held, I., Kushnir, Y., Lu, J., Vecchi, G., Huang, H.-P., Harnik, N., Leetmaa, A., Lau, N.-C., Li, C., Velez, J., Naik, N., 2007. Model projections of an imminent transition to a more arid climate in southwestern North America. Science 316 (5828), 1181–1184. https://doi.org/10.1126/science.1139601.

Seager, R., Ting, M., Li, C., Naik, N., Cook, B., Nakamura, J., Liu, H., 2013. Projections of declining surface-water availability for the southwestern United States. Nat. Clim. Change 3 (5), 482–486 letter.

Stöckli, R., Lawrence, D.M., Niu, G.-Y., Oleson, K.W., Thornton, P.E., Yang, Z.-L., Bonan, G.B., Denning, A.S., Running, S.W., 2008. Use of FLUXNET in the Community Land Model development. J. Geophys. Res. Biogeosci. 113 (G1). https://doi.org/10.1029/2007JG000562. G01,025.

Swann, A.L.S., Hoffman, F.M., Koven, C.D., Randerson, J.T., 2016. Plant responses to increasing CO_2 reduce estimates of climate impacts on drought severity. Proc. Natl. Acad. Sci. 113 (36), 10019–10024. https://doi.org/10.1073/pnas.1604581113.

Trenberth, K.E., Dai, A., Van Der Schrier, G., Jones, P.D., Barichivich, J., Briffa, K.R., Sheffield, J., 2014. Global warming and changes in drought. Nat. Clim. Change 4 (1), 17–22.

Trugman, A.T., Medvigy, D., Mankin, J.S., Anderegg, W.R.L., 2018. Soil moisture stress as a major driver of carbon cycle uncertainty. Geophys. Res. Lett. 45 (13), 6495–6503. https://doi.org/10.1029/2018GL078131.

Urbanski, S., Barford, C., Wofsy, S., Kucharik, C., Pyle, E., Budney, J., McKain, K., Fitzjarrald, D., Czikowsky, M., Munger, J.W., 2007. Factors controlling CO_2 exchange on timescales from hourly to decadal at Harvard Forest. J. Geophys. Res. Biogeosci. 112 (G2), g02020. https://doi.org/10.1029/2006JG000293.

Watts, D.G., Bacon, D.W., 1974. Using an hyperbola as a transition model to fit two-regime straight-line data. Technometrics 16 (3), 369–373. https://doi.org/10.1080/00401706.1974.10489205.

Wellstein, C., Poschlod, P., Gohlke, A., Chelli, S., Campetella, G., Rosbakh, S., Canullo, R., Kreyling, J., Jentsch, A., Beierkuhnlein, C., 2017. Effects of extreme drought on specific leaf area of grassland species: a meta-analysis of experimental studies in temperate and sub-Mediterranean systems. Global Change Biol. 23 (6), 2473–2481. https://doi.org/10.1111/gcb.13662.

Wuebbles, D., Meehl, G., Hayhoe, K., Karl, T.R., Kunkel, K., Santer, B., Wehner, M., Colle, B., Fischer, E.M., Fu, R., Goodman, A., Janssen, E., Kharin, V., Lee, H., Li, W., Long, L.N., Olsen, S.C., Pan, Z., Seth, A., Sheffield, J., Sun, L., 2014. CMIP5 climate model analyses: climate extremes in the United States. Bull. Am. Meteorol. Soc. 95 (4), 571–583. https://doi.org/10.1175/BAMS-D-12-00172.1.

Xu, L., Baldocchi, D.D., 2004. Seasonal variation in carbon dioxide exchange over a Mediterranean annual grassland in California. Agric. Forest Meteorol. 123 (1), 79–96. https://doi.org/10.1016/j.agrformet.2003.10.004.

Zhao, M., Running, S., 2010. Drought-induced reduction in global terrestrial net primary production from 2000 through 2009. Science 329 (5994), 940.